Published for SISSA by Springer

Received: November 25, 2013
Revised: May 13, 2014
Accepted: June 6, 2014
Published: June 26, 2014

Weighing the light gravitino mass with weak lensing surveys

Ayuki Kamada,[a] **Masato Shirasaki**[b] **and Naoki Yoshida**[a,b]

[a] *Kavli IPMU (WPI), University of Tokyo, Chiba 277-8583, Japan*

[b] *Department of Physics, University of Tokyo, Tokyo 113-0033, Japan*

E-mail: ayuki.kamada@ipmu.jp, masato.shirasaki@utap.phys.s.u-tokyo.ac.jp, naoki.yoshida@phys.s.u-tokyo.ac.jp

Abstract: We explore the discovery potential of light gravitino mass $m_{3/2}$ by combining future cosmology surveys and collider experiments. The former probe the imprint of light gravitinos in the cosmic matter density field, whereas the latter search signatures of a supersymmetry breaking mechanism. Free-streaming of light gravitinos suppresses the density fluctuations at galactic and sub-galactic length scales, where weak gravitational lensing can be used as a powerful probe. We perform numerical simulations of structure formation to quantify the effect. We then run realistic ray-tracing simulations of gravitational lensing to measure the cosmic shear in models with light gravitino. We forecast the possible reach of future wide-field surveys by Fisher analysis; the light gravitino mass can be determined with an accuracy of $m_{3/2} = 4 \pm 1\,\mathrm{eV}$ by a combination of the Hyper Suprime Cam survey and cosmic microwave background anisotropy data obtained by Planck satellite. The corresponding accuracy to be obtained by the future Large Synoptic Survey Telescope is $\delta m_{3/2} = 0.6\,\mathrm{eV}$. Data from experiments at Large Hadron Collider at 14 TeV will provide constraint at $m_{3/2} \simeq 5\,\mathrm{eV}$ in the minimal framework of gauge-mediated supersymmetry breaking (GMSB) model. We conclude that a large class of the GMSB model can be tested by combining the cosmological observations and the collider experiments.

Keywords: Cosmology of Theories beyond the SM, Supersymmetry Breaking, Supersymmetric Standard Model

ArXiv ePrint: 1311.4323

doi:10.1007/JHEP06(2014)162

JHEP06(2014)162

Contents

1 Introduction **1**

2 SUSY particle masses in the GMSB model **3**

3 Linear evolution of density perturbations with light gravitino **4**

4 Weak gravitational lensing **6**
- 4.1 Lensing power spectrum 6
- 4.2 Cosmological simulations 8
  - 4.2.1 N-body simulations 8
  - 4.2.2 Ray-tracing simulation 8

5 Results **9**
- 5.1 Convergence power spectrum 9
- 5.2 Fisher analysis 11
- 5.3 Forecast for future surveys 13
- 5.4 Degeneracy between light gravitino and massive neutrino 14

6 Summary and discussion **15**

JHEP06(2014)162

1 Introduction

Supersymmetry (SUSY) is one of the most attractive candidates of physics beyond the standard model. Minimal supersymmetric extension of the standard model (MSSM, see e.g. [1]) with $\sim \mathcal{O}$(TeV) SUSY particles can possibly address several important issues in the standard model, such as the large hierarchy between the electro-weak scale and the grand unification scale, the existence of dark matter, and the origin of the cosmic baryon number. The MSSM is also known to achieve successful grand unification of the standard model gauge couplings at some high energy.

The null-detection of the SUSY particles so far suggests that SUSY is broken at some energy scale and mediated to MSSM via some messenger. Several mechanisms are proposed as the messenger such as gravity-mediated, anomaly-mediated, and gauge-mediated SUSY breaking (GMSB) models. GMSB models generally evade the flavor changing neutral current problem and the CP-problem, and thus they are thought to be the most interesting models.

Supergravity (SUGRA) as an extension of the global SUSY to the local one involves the superpartner of the graviton, which is referred to gravitino. The gravitino has helicity

$\pm 3/2$ and obtains the mass via the super-Higgs mechanism:

$$m_{3/2} = \frac{|\langle F \rangle|}{\sqrt{3} M_{\rm pl}} \,, \tag{1.1}$$

with the vacuum expectation value of F-term $\langle F \rangle$ and the reduced Planck mass $M_{\rm pl} \simeq 2.43 \times 10^{18}\,{\rm GeV}$. The gravitino is produced in the thermal bath immediately after the reheating of the Universe through the F-term suppressed interaction of goldstino component with spin $\pm 1/2$.

In the GMSB models, the gravitino mass is predicted to be in the range of $m_{3/2} \sim$ eV-keV. The small F-term allows the gravitino to be in the thermal equilibrium until the decoupling of others SUSY particles. When the gravitino is decoupled from the thermal bath, it begins to stream freely and contributes as a "diffuse" matter component of the Universe. The gravitino free-streaming imprints characteristic features on the matter power spectrum, which are expected to be probed by observations of large-scale structure. For example, the current constraint of $m_{3/2} < 16\,{\rm eV}$ is obtained by measuring the Ly-α flux power spectra that essentially probe the distribution of the inter-galactic medium at high redshifts [2]. We note that the constraint is based on the crucial assumption that the distribution of the inter-galactic neutral gas traces the distribution of underlying dark matter even at nonlinear length scales. Gravitational lensing provides a direct physical means of probing the distribution of total matter. For example, it has been suggested that cosmic microwave background lensing has a potential to probe the gravitino mass of $m_{3/2} \simeq 1\,{\rm eV}$ in future experiments [3].

While the cosmological observations place an upper bound on the gravitino mass, the terrestrial collider experiments such as on-going Large Hadron Collider (LHC) give a lower bound through signatures of other SUSY particles (see section 2). In the present paper, we show that essentially all the interesting range of the gravitino mass can be probed by combining the up-coming LHC run at 14 TeV and the near future weak lensing surveys by the Subaru Hyper Suprime-Cam (HSC) and the Large Synoptic Survey Telescope (LSST).

Gravitational lensing is one of the powerful tools to probe directly the matter distribution in the Universe. The coherent pattern of image distortion by weak lensing is called cosmic shear. Cosmic shear in principle can be induced by any foreground mass distribution along the line of sight regardless of its dynamical state or luminosity. Cosmic shear signals have been detected with high significance levels, and constraints on some basic cosmological parameters have been derived [4–7]. Upcoming weak lensing surveys such as HSC will cover a wide area extending more than a thousand square degrees. The surveys will also probe the matter distribution at mega-parsec length scale most accurately, where the imprints of the gravitino can be detected. It is therefore important and timely to study the effect of the light gravitino on cosmic shear. To this end, we run a set of cosmological N-body simulations to follow the nonlinear evolution of the matter density fluctuations with the imprints of the gravitino free-streaming. We then perform accurate ray-tracing simulations of gravitational lensing. We show that the cosmic shear is indeed a promising probe of the existence and the mass of the light gravitino.

JHEP06(2014)162

The rest of the paper is organized as follows. In section 2, we introduce the basics of the GMSB model. In particular, we clarify the relation between the gravitino mass and the masses of other SUSY particles. In section 3, we discuss the linear evolution of the primordial density perturbation under the effect of the light gravitino. We present the resulting linear matter power spectra, which provides the initial conditions for our cosmological N-body simulations. In section 4, we describe our simulation set-ups. In section 5, we measure the cosmic shear power spectra from the simulations and forecast the discovery potential of the light gravitino in the future weak lensing surveys. The final section is devoted to the concluding remarks.

2 SUSY particle masses in the GMSB model

In the GMSB models [8–13], the SUSY breaking is mediated from the hidden sector to the MSSM sector via some messenger fields that are charged under the standard model gauge group. The gaugino and the sfermion masses are induced by the one-loop and the two-loop diagrams, respectively, at the leading order. Note that the gaugino and sfermion mass spectrum generically depends on the charge assignment to the messenger fields and that inadequate charge assignment might ruin the success of MSSM in the grand unification of the gauge couplings. A popular choice is to set messenger fields in complete multiplets of the SU(5) global/gauge symmetry. In the rest of this section, we consider specifically one of such models, the so-called minimal GMSB model.

The minimal GMSB model has the superpotential of

$$W = (\lambda S + M) \sum_{n=1}^{N_5} \Phi_n \bar{\Phi}_n \,, \tag{2.1}$$

where S is the goldstino superfields and M is the messenger mass. The F-term of the goldstino superfields develops the vacuum expectation values $\langle F \rangle$, and the N_5 pairs of messenger superfields Φ_n and $\bar{\Phi}_n$ $(n = 1, \ldots, N_5)$ form the multiplets of $\mathbf{5}$ and $\bar{\mathbf{5}}$ of SU(5). In the minimal GMSB model, the gaugino mass is given by,

$$M_a = \frac{g_a^2}{16\pi^2} \Lambda N_5 g(x), \tag{2.2}$$

where the index $a\,(= 1, 2, 3)$ corresponds to the standard model gauge group $\mathrm{U}(1)_Y \times \mathrm{SU}(2)_L \times \mathrm{SU}(3)_C$, and g_a denotes the standard model gauge coupling. We normalize g_1 and g_2 such that $g_1 = \sqrt{5/3}\, g'$ and $g_2 = g$ with the conventional electro-weak gauge couplings g and g' ($e = g \sin\theta_W = g' \sin\theta_W$, e: positron charge, θ_W: Weinberg angle). The messenger scale Λ is defined by,

$$\Lambda = \left| \frac{\lambda \langle F \rangle}{M} \right| . \tag{2.3}$$

The function $g(x)$ is given by,

$$g(x) = \frac{1}{x^2}(1+x)\ln(1+x) + (x \to -x)\,, \tag{2.4}$$

JHEP06(2014)162

and its argument is the dimensionless parameter $x = |\Lambda/M|$. The sfermion mass squared is given by

$$m_{\phi_i}^2 = 2\Lambda^2 N_5 \sum_{a=1}^{3} C_a(i) \left(\frac{g_a^2}{16\pi^2}\right)^2 f(x)\,, \tag{2.5}$$

where the index i denotes fermion flavour and $C_a(i)$ is the Casimir invariant. The function $f(x)$ is given by,

$$f(x) = \frac{1+x}{x^2}\left[\ln(1+x) - 2\mathrm{Li}_2\left(\frac{x}{1+x}\right) + \frac{1}{2}\mathrm{Li}_2\left(\frac{2x}{1+x}\right)\right] + (x \to -x)\,, \tag{2.6}$$

with the dilogarithm function $\mathrm{Li}_2(x)$. In practice, we use the public code `softsusy` [14] to calculate the mass spectrum of SUSY particles numerically. The calculations take into account the renormalization group running of SUSY particle masses. The gravitino mass (eq. (1.1)) can be written in terms of the GMSB variables,

$$m_{3/2} = \frac{\Lambda M}{\sqrt{3} M_{\rm pl}|\lambda|} = \frac{\Lambda^2}{\sqrt{3} M_{\rm pl}|\lambda| x}\,. \tag{2.7}$$

From eqs. (2.2), (2.5) and (2.7), we can see that the SUSY particle masses are proportional to the square root of the gravitino mass, M_a, $m_{\phi_i} \propto \Lambda \propto \sqrt{m_{3/2}}$. Therefore, collider experiments with higher energies can be used generally to search for signatures of heavier SUSY particles, which in turn give information on gravitinos with relatively larger masses. Note that, in high-energy collision of the standard model particles, the direct product is not gravitino with gravitational interaction, but other SUSY particles with gauge interaction. For example, in proton-proton collision experiments at the LHC, the colored SUSY particles (i.e. gluino and squarks) are important and directly related to the discovery potential for SUSY particles. Lighter gravitinos are associated with lighter colored SUSY particles that can be searched even with the current generation experiments.

The LHC current and future reach for the GMSB models is studied in detail in [15–23]. It is generally model-dependent to connect masses of heavier SUSY particles and mass of the light gravitino. Specifically the collider lower bound on the light gravitino mass depends on properties of the messenger and hidden sectors, N_5 and λx in the case of the minimal GMSB model as we can see from eqs. (2.2), (2.5) and (2.7). In order to derive specific constraints, we discuss the LHC constraints in section 5 by taking some specific focus point in the minimal GMSN model.

3 Linear evolution of density perturbations with light gravitino

The light gravitino is in thermal equilibrium immediately after the reheating of the Universe unless the reheating temperature is extremely low [26]. When the cosmic temperature drops below the other SUSY particle masses, the decay and inverse-decay processes that have been keeping the thermal equilibrium between the light gravitino and the thermal bath, become inefficient. Then the light gravitino particles begin to stream freely with the momenta following the Fermi-Dirac distribution.

JHEP06(2014)162

The gravitino contribution to the cosmic energy density is given by,

$$\Omega_{3/2}h^2 = 0.13 \left(\frac{g_{3/2}}{2}\right) \left(\frac{m_{3/2}}{100\,\mathrm{eV}}\right) \left(\frac{g_{*s3/2}}{90}\right)^{-1} \tag{3.1}$$

where $g_{*s3/2}$ is the effective massless degrees of freedom for the cosmic entropy at the time of gravitino decoupling. The exact value of $g_{*s3/2}$ depends on the mass spectrum of the SUSY particles (e.g. Λ) [3, 27]. However, its weak dependence allows us to fix $g_{*s3/2} = 90$ without changing our results by more than 5 %. It should be noted that the effective internal degrees of freedom of gravitino is not $g_{3/2} = 4$, but $g_{3/2} = 2$. This is because only goldstino component (spin $\pm 1/2$) can interact with the thermal bath through the $1/\langle F\rangle$ suppressed interactions.

From the above formula, we find that the light gravitino with $m_{3/2} \lesssim 100\,\mathrm{eV}$ (of our interest here) cannot account for the cosmological dark matter mass density. We assume that some cold and stable particle makes up the rest of dark matter, i.e.,

$$\Omega_{\mathrm{dm}} = \Omega_{\mathrm{cs}} + \Omega_{3/2}\,. \tag{3.2}$$

Such a cold and stable particle can be, e.g., the QCD axion [28–30] or the composite baryons generated in the SUSY breaking/messenger sector in models with strongly coupled low scale gauge mediation [31–34].

The free-streaming of light gravitino affects the evolution of primordial density perturbations in a similar manner as the standard model neutrinos do. We discuss the similarity and indeed the degeneracy of the effects of the light gravitino and the standard model neutrinos later in section 5. The suppression owing to free-streaming occurs below a cut-off scale that is characterized by the Jeans scale at the matter-radiation equality a_{eq} [35]:

$$k_{\mathrm{J}} = a\sqrt{\frac{4\pi G\rho_{\mathrm{M}}}{\langle v^2\rangle}}\bigg|_{a=a_{\mathrm{eq}}} \simeq 0.86\,\mathrm{Mpc}^{-1} \left(\frac{g_{3/2}}{2}\right)^{-1/2} \left(\frac{m_{3/2}}{100\,\mathrm{eV}}\right)^{1/2} \left(\frac{g_{*s3/2}}{90}\right)^{5/6}, \tag{3.3}$$

where G is the Newton's constant and ρ_{M} is the total matter density of the Universe. The mean square velocity $\langle v^2\rangle$ is evaluated over the whole dark matter mass distribution function $f_{\mathrm{dm}}(v)$ ($\int d^3v f_{\mathrm{dm}}(v) = \rho_{\mathrm{dm}}$). It means $\langle v^2\rangle = f_{3/2}\,\langle v^2\rangle_{3/2}$ effectively, where $f_{3/2}$ is the gravitino density fraction ($f_{3/2} \equiv \Omega_{3/2}/\Omega_c$) and $\langle v^2\rangle_{3/2}$ is the mean square velocity of the gravitino particles. The resultant linear matter power spectrum is shown and compared with that of the standard ΛCDM model in figure 1.

Before discussing the details of the matter power spectrum, let us briefly consider the effect of some non-standard thermal history of the Universe. The overall influence of the light gravitino on the cosmic expansion can be basically characterized by one parameter, the gravitino mass $m_{3/2}$. This is because the gravitino temperature of the Fermi-Dirac distribution can be related to the observed CMB temperature through entropy conservation, i.e. $g_{*s3/2} \simeq 90$. However, non-standard thermal history with, e.g., entropy production [36], can change $g_{*s3/2}$ drastically to $g_{*s3/2} \simeq \mathcal{O}(1000)$. Then cosmological constraint on $m_{3/2}$ can be significantly altered, or the constraint needs to be re-interpreted within a suitable class of models. In the following discussion, we consider the standard thermal history with $g_{*s3/2} = 90$, and hence $m_{3/2}$ is the single model parameter.

JHEP06(2014)162

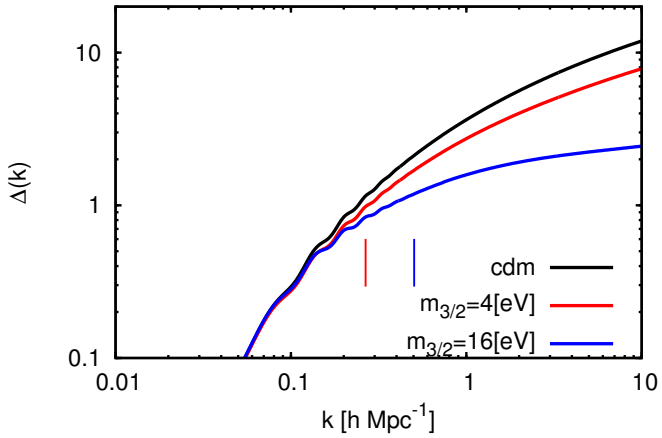

Figure 1. Linear dimensionless matter power spectra for $m_{3/2} = 0\,(\text{cdm})$, 4, and 16 eV. We adopt basic cosmological parameters given by the Planck mission first year results [38]. The vertical lines represent the cut-off scales of eq. (3.3).

We calculate the evolution of the linear density perturbation δ by modifying `CAMB` [37] suitably. In figure 1, we plot the dimensionless matter power spectra $\Delta(k)$ defined by

$$\langle \delta(\mathbf{x})\delta(\mathbf{y})\rangle = \int d\ln k\, \Delta(k)\, e^{i\mathbf{k}\cdot(\mathbf{x}-\mathbf{y})}\,, \tag{3.4}$$

for mixed dark matter models with $m_{3/2} = 0\,(\text{cdm})$, 4, and 16 eV. We adopt the cosmological parameters of the Planck mission first year results [38]. The free-streaming effect appears clearly at small length scales (eq. (3.3)) but the suppression below the cut-off scale is more significant for models with heavier gravitino (compare $m_{3/2} = 4\,\text{eV}$ and 16 eV in figure 1). This is because larger $m_{3/2}$ gives a larger fractional contribution to the total matter density as $f_{3/2} \propto m_{3/2}$. We thus expect that models with heavy gravitino can be constrained by observations of large-scale structure of the universe.

4 Weak gravitational lensing

4.1 Lensing power spectrum

We summarize basics of gravitational lensing by large-scale structure. When one denotes the observed position of a source object as $\boldsymbol{\theta}$ and the true position as $\boldsymbol{\beta}$, one can characterize the distortion of image of a source object by the following 2D matrix:

$$A_{ij} = \frac{\partial\beta^i}{\partial\theta^j} \equiv \begin{pmatrix} 1-\kappa-\gamma_1 & -\gamma_2 \\ -\gamma_2 & 1-\kappa+\gamma_1 \end{pmatrix}, \tag{4.1}$$

where κ is convergence and γ is shear. In weak lensing regime (i.e. $\kappa, \gamma \ll 1$), each component of A_{ij} can be related to the second derivative of the gravitational potential

JHEP06(2014)162

Φ [39, 40] as

$$A_{ij} = \delta_{ij} - \Phi_{ij}, \tag{4.2}$$

$$\Phi_{ij} = \frac{2}{c^2}\int_0^{\chi} \mathrm{d}\chi' g(\chi,\chi')\frac{\partial^2}{\partial x_i \partial x_j}\Phi[r(\chi')\boldsymbol{\theta},\chi'], \tag{4.3}$$

$$g(\chi,\chi') = \frac{r(\chi-\chi')r(\chi')}{r(\chi)} \tag{4.4}$$

where χ is comoving distance, $r(\chi)$ is angular diameter distance, and $x_i = r\theta_i$ represents physical distance. By using the Poisson equation, one can relate the convergence field to the matter overdensity field δ [39, 40]. Weak lensing convergence field is then given by

$$\kappa(\boldsymbol{\theta},\chi) = \frac{3}{2}\left(\frac{H_0}{c}\right)^2 \Omega_{\mathrm{m0}}\int_0^{\chi}\mathrm{d}\chi' g(\chi,\chi')\frac{\delta[r(\chi')\boldsymbol{\theta},\chi']}{a(\chi')}. \tag{4.5}$$

In this paper, we use the convergence power spectrum to constrain the gravitino mass. With the flat sky approximation, which is sufficient for angular scales of our interest, the Fourier transform of convergence field is defined by

$$\kappa(\boldsymbol{\theta}) = \int \frac{\mathrm{d}^2\ell}{(2\pi)^2} e^{i\boldsymbol{\ell}\cdot\boldsymbol{\theta}}\tilde{\kappa}(\boldsymbol{\ell}). \tag{4.6}$$

The power spectrum of the convergence field P_κ is defined by

$$\langle\tilde{\kappa}(\boldsymbol{\ell}_1)\tilde{\kappa}(\boldsymbol{\ell}_2)\rangle = (2\pi)^2\delta_D(\boldsymbol{\ell}_1-\boldsymbol{\ell}_2)P_\kappa(\ell_1), \tag{4.7}$$

where $\delta_D(\boldsymbol{\ell})$ is the Dirac delta function. By using Limber approximation [41, 42] and eq. (4.5), we obtain the convergence power spectrum as

$$P_\kappa(\ell) = \int_0^{\chi_s}\mathrm{d}\chi\frac{W(\chi)^2}{r(\chi)^2}P_\delta\left(k=\frac{\ell}{r(\chi)},z(\chi)\right), \tag{4.8}$$

where $P_\delta(k)$ is the three dimensional matter power spectrum, χ_s is comoving distance of source galaxies and $W(\chi)$ is the lensing weight function defined as

$$W(\chi) = \frac{3}{2}\left(\frac{H_0}{c}\right)^2\Omega_{\mathrm{m0}}\frac{r(\chi_s-\chi)r(\chi)}{r(\chi_s)}(1+z(\chi)). \tag{4.9}$$

The non-linear gravitational growth of $P_\delta(k)$ significantly affects the amplitude of convergence power spectrum for the angular scales less than 1 degree [43–45]. Typical weak lensing surveys are aimed at measuring the cosmic shear at angular scales larger than a few arcmin, corresponding to a few mega-parsec. Therefore, accurate theoretical prediction of non-linear matter power spectrum is essential to derive cosmological constraints from weak lensing power spectrum. Several analytic models are available that accurately predict the non-linear evolution of $P_\delta(k)$ for the standard ΛCDM universe [46–49]. Unfortunately, there are no calibrated fitting formulae of $P_\delta(k)$ for the mixed dark matter models we consider here. We thus use direct numerical simulations to obtain the convergence power spectra.

JHEP06(2014)162

	$m_{3/2}$ [eV]	$z_{\rm init}$	# of N-body sims
CDM	0	49	5
MDM4–lowz	4	9	5
MDM16–lowz	16	9	5
MDM4–highz	4	49	5
MDM16–highz	16	49	5

Table 1. Parameters for our N-body simulations. For each model, we run 5 N-body realizations and generate 20 weak lensing convergence maps.

4.2 Cosmological simulations

4.2.1 N-body simulations

It is necessary to use ray-tracing simulations in order to study the effect of light gravitino on the weak lensing power spectrum in nonlinear regimes. We first run cosmological N-body simulations for models with light gravitinos. We use the parallel Tree-Particle Mesh code `Gadget2` [50]. Each simulation is run with 512^3 dark matter particles in a volume of comoving 240 Mpc/h on a side. We generate the initial conditions following the standard Zel'dovich approximation. We use the accurate linear matter power spectrum calculated by the modified `CAMB` (section 3). It is important to generate the initial conditions at a sufficiently low redshift so that the total matter, including the contribution from the light gravitino, can be treated as effectively a cold component. We set the initial redshift $z_{\rm init} = 9$ because the typical thermal velocity of the gravitino is then sufficiently small compared to the virial velocity of the smallest halos resolved in our simulation. We also run a N-body simulation from $z_{\rm init} = 49$ for the mixed dark matter model to examine the overall effect caused by the choice of $z_{\rm init}$.

For our fiducial cosmology, we adopt the following parameters: matter density $\Omega_m = 0.3175$, dark energy density $\Omega_\Lambda = 0.6825$ with the equation of state parameter $w_0 = -1$, Hubble parameter $h = 0.6711$ and the primordial spectrum with the scalar spectral index $n_s = 0.9624$ and the normalized amplitude $A_s = 2.215 \times 10^{-9}$ at the pivot scale $k = 0.05\,{\rm Mpc}^{-1}$. These parameters are consistent with the Planck mission first year results [38]. Two cases with the gravitino mass $m_{3/2} = 4$ and 16 eV are chosen as representative models. We summarize the simulation parameters in table 1.

4.2.2 Ray-tracing simulation

We generate light-cone outputs from our N-body simulations for ray-tracing simulations of gravitational lensing. The simulation boxes are placed to cover a past light-cone of a hypothetical observer with angular extent $5^\circ \times 5^\circ$, from redshift $z = 0$ to $z \sim 1$, similarly to the methods in [51, 52]. We use the standard multiple lens plane algorithm in order to simulate gravitational lensing signals [43]. The configuration of our simulations is similar to that in [45].

We set the initial ray directions on 4096^2 grids. The corresponding angular grid size is $5^\circ/4096 \sim 0.075$ arcmin. To avoid multiple appearance of the same structure aligned

JHEP06(2014)162

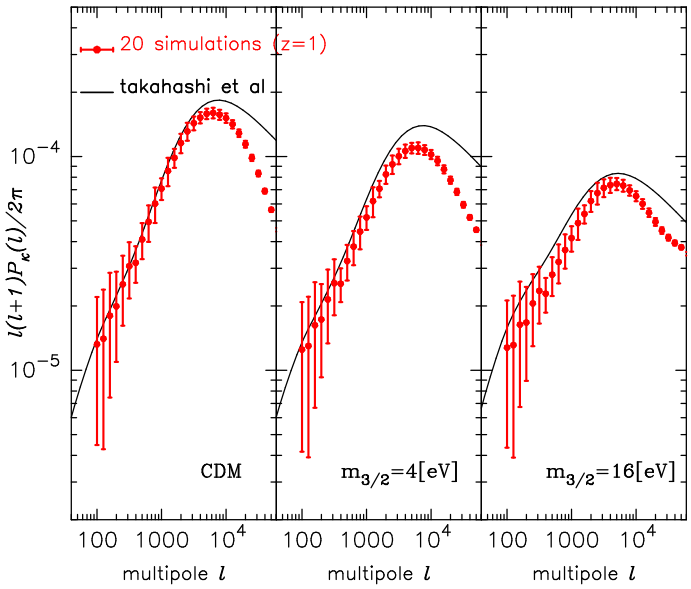

Figure 2. The convergence power spectra from our ray-tracing simulations for models with $m_{3/2} = 0, 4$ and 16 eV are shown in the left, medium and right panels, respectively. In each panel, the red points represent the average measured power spectrum and the error bars show the standard deviation over 20 realizations. We use the simulations that start from $z_{\rm init} = 9$ for this figure. The solid line is calculated by eq. (4.8) and fitting formula of $P_\delta(k)$ in [49] with $z_{\rm source} = 1.0$.

along a line-of-sight, we shift randomly the N-body simulation boxes. In addition, we use simulation outputs from independent realizations when generating the light-cone outputs. Finally we obtain 20 independent convergence maps from 5 N-body simulations for each cosmological model. We fix the redshift of the source galaxies to $z_{\rm source} = 1.0$.

We measure the binned power spectrum of convergence field by averaging the product of Fourier modes $|\tilde{\kappa}(\boldsymbol{\ell})|^2$ for each multiple bin with $\Delta \log_{10} \ell = 0.1$ from $\ell = 100$ to 10^5.

5 Results

5.1 Convergence power spectrum

Let us first discuss how the light gravitino affects the lensing power spectrum. Figure 2 compares the measured convergence power spectra with the analytic model prediction (eq. (4.8)) calculated by the fitting model in [49]. The results for $m_{3/2} = 0, 4$ and 16 eV are shown in the left, medium and right panels, respectively. The red points show the average power spectrum over 20 realizations with the error bars indicating the standard deviation of the realizations. The solid line is the model prediction of eq. (4.8) for $z_{\rm source} = 1$. Note that the fitting function for $P_\delta(k)$ is calibrated for the standard ΛCDM cosmologies with a wide range of cosmological parameters. We thus assume that the non-linear evolution of $P_\delta(k)$ for our mixed dark matter model is also described in the same manner as in the standard ΛCDM. In practice, we simply input the linear power spectrum for the mixed dark matter model (section 3), but do not change the coefficients in the formula.

JHEP06(2014)162

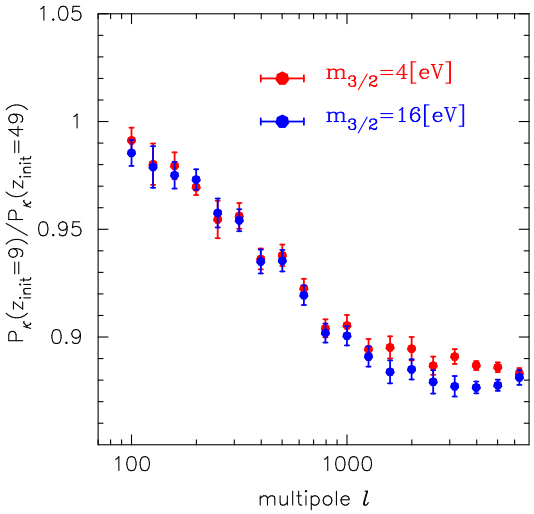

Figure 3. We plot the ratio of the lensing power spectra of the ray-tracing simulations with $z_{\rm init} = 9$ and 49. The error bars indicating standard deviation estimated from 20 realizations.

We see in figure 2 that the analytic model and the simulation result agree well to $\ell \leq 4000$. This is consistent with the results of previous studies [45, 49]; the fitting model becomes less accurate at (sub-)arcminute scales even in the case of standard ΛCDM cosmology. The convergence power spectra for the mixed dark matter model differ significantly from that for the ΛCDM model even at around $\ell = 1000$ corresponding to physical megaparsec scale. Clearly, free-streaming of the gravitino affects the matter power spectrum at the nonlinear scales, and thus the above simple analytic approach does not work well even at $\ell = 1000$ for the mixed dark matter model.

We have examined the effect of choice of the initial redshift. In general, N-body simulations for the kind of mixed dark matter model should be initialized at a sufficiently low redshift in order to avoid numerical effects owing to gravitino thermal motions. Because assigning thermal velocities to N-body simulation particles is a non-trivial issue (see, e.g., [53]), we do not attempt to add random velocities to the particles. Instead, we examine how the choice of initial redshift affects the result at low redshifts by comparing two simulations that are started from $z_{\rm init} = 9$ and 49. Figure 3 compares the lensing power spectra obtained from our simulations with different $z_{\rm init}$.

The red points are for the gravitino with $m_{3/2} = 4\,\mathrm{eV}$ and the blue points for $m_{3/2} = 16\,\mathrm{eV}$. Note that, unlike in ordinary warm dark matter models, the free-streaming scale, the gravitino mass, and the cosmic abundance are all related to each other in our light gravitino model. We plot the standard deviation of mean value over 20 maps as error bars for each model. We find that the initial redshift affects the convergence power spectra at a level of $\sim 10\,\%$. It is important to note that the simulation from $z_{\rm init} = 49$ is not set up consistently, because our simulation particles can represent only non-relativistic components, while the light gravitino is relativistic at such a high redshift. Overall, figure 3 indicates that the simulated lensing power spectrum for the mixed dark matter model likely has inaccuracies with a level of $\sim 10\%$.

JHEP06(2014)162

	$m_{3/2}$ [eV]	$10^9 A_s$	n_s	$\Omega_c h^2$	w_0
fiducial	4	2.215	0.924	0.12029	-1
$d\boldsymbol{p}$	–	0.1	0.01	0.03	0.1

Table 2. Parameters in our Fisher analysis. For each parameter, we calculate the power spectra P_κ with $d\boldsymbol{p}$ varied around the fiducial value in order to calculate the derivative of equation (5.2).

5.2 Fisher analysis

We perform a Fisher analysis to forecast the cosmological parameter constraints, including $m_{3/2}$. For a multivariate Gaussian likelihood, the Fisher matrix F_{ij} is written as

$$F_{ij} = \frac{1}{2}\mathrm{Tr}\left[A_i A_j + C^{-1}M_{ij}\right], \tag{5.1}$$

where $A_i = C^{-1}\partial C/\partial p_i$, $M_{ij} = 2\left(\partial P_\kappa/\partial p_i\right)\left(\partial P_\kappa/\partial p_j\right)$, C is the data covariance matrix and $\boldsymbol{p}$ is a set of parameters of interest.[1] In the present study, we choose $\boldsymbol{p} = (m_{3/2}, 10^9 A_s, n_s, \Omega_c h^2, w_0)$ as cosmological parameters to constrain. For the Fisher analysis, we need to calculate the derivative of P_κ with respect to $\boldsymbol{p}$. For $m_{3/2}$, we first fit the measured power spectrum $P_\kappa(\ell)$ using a quadratic form of $m_{3/2}$, i.e. $a_0(\ell) + a_1(\ell)m_{3/2} + a_2(\ell)m_{3/2}^2$. We then calculate the derivative by $a_1(\ell) + 2a_2(\ell)m_{3/2}$. For the other parameters, we evaluate the derivatives as follows:

$$\frac{\partial P_\kappa(\ell)}{\partial p_i} = \frac{P_\kappa(\ell, p_i^{(0)} + dp_i) - P_\kappa(\ell, p_i^{(0)} - dp_i)}{2dp_i}, \tag{5.2}$$

where $p_i^{(0)}$ is the fiducial value and dp_i is the variation of i-th parameter. Here, we simply calculate $P_\kappa(\ell, \boldsymbol{p})$ using eq. (4.8) and the fitting formula of $P_\delta(k)$ in [49]. We summarize the fiducial values of $\boldsymbol{p}$ and $d\boldsymbol{p}$ in table 2.

The covariance matrix of the convergence power spectrum can be expressed as a sum of the Gaussian and non-Gaussian contributions [45, 55]. Previous studies show that the non-Gaussian error degrades the constraints on cosmological parameters with a level of $O(10\%)$ [56]. We calculate the non-Gaussian contribution by using 1000 lensing maps in [45] in the following direct manner:

$$\mathrm{Cov}[P_\kappa(\ell), P_\kappa(\ell')] = \frac{1}{N_R - 1}\sum_{r=1}^{N_R}(\hat{P}_\kappa^r(\ell) - \bar{P}_\kappa(\ell))(\hat{P}_\kappa^r(\ell') - \bar{P}_\kappa(\ell')), \tag{5.3}$$

where $\hat{P}_\kappa^r(\ell)$ is the measured power spectrum in r-th realization and $\bar{P}_\kappa(\ell)$ is the average power spectrum over $N_R = 1000$ realizations. The configuration of the simulation in [45] is similar to ours, which covers 25 deg^2 on the sky. When necessary, we simply scale the covariance matrix eq. (5.3) by the designated survey area.

We also take various systematic effects into account in the following manner. It is well-known that the intrinsic ellipticities of source galaxies induce noises to lensing power

[1] We only consider the second term in eq. (5.1). Because C scales approximately inverse-proportionally to survey area, the second term is expected to be dominant for a very wide area survey [54].

JHEP06(2014)162

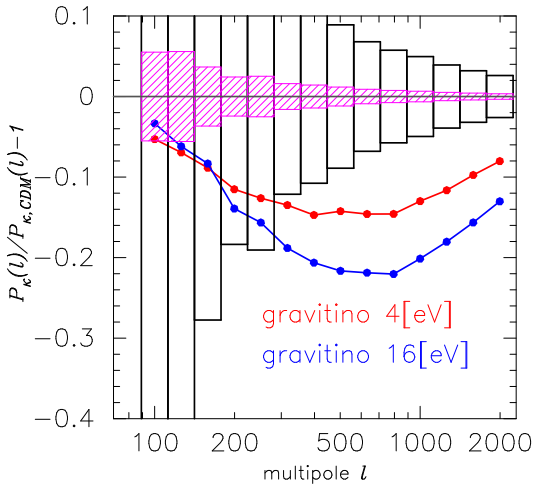

Figure 4. The derived statistical error of the lensing power spectrum. The boxes show the statistical error of lensing power spectrum given by a sum of eq. (5.3) and (5.4). The black boxes are for a 25 deg^2 area survey, which is same as the size of our simulation. The purple hatched regions show the expected error for upcoming lensing survey with an area of 1500 deg^2. For comparison, we also plot the difference of the lensing power spectra between the pure CDM model and mixed dark matter models. The red line is for $m_{3/2} = 4\,\mathrm{eV}$ and the blue one for $m_{3/2} = 16\,\mathrm{eV}$. For this plot, the number density of sources is set to be 10 arcmin^{-2}.

spectrum. Assuming intrinsic ellipticities are uncorrelated, we compute the noise contribution to the covariance matrix of convergence power spectrum as [57]

$$\mathrm{Cov}[P_\kappa(\ell), P_\kappa(\ell')]|_{\mathrm{noise}} = \frac{2}{f_{\mathrm{sky}}(2\ell+1)\Delta\ell} P_{\mathrm{noise}} \left(P_{\mathrm{noise}} + 2P_\kappa(\ell)\right) \delta_{\ell\ell'}, \tag{5.4}$$

$$P_{\mathrm{noise}} = \frac{1}{n_{\mathrm{gal}}} \left(\frac{\sigma_{\mathrm{int}}}{\mathcal{R}}\right)^2, \tag{5.5}$$

where $\Delta\ell$ is the width of the multipole bin, f_{sky} is the fraction of sky covered, n_{gal} is the number density of source galaxies, $\mathcal{R}$ is the shear response, and σ_{int} is the root-mean-square of the shear noise. Throughout the present paper, we adopt $\mathcal{R} = 1.7$ and $\sigma_{\mathrm{int}} = 0.4$. The values are typical in ground based weak lensing surveys [58, 59]. We finally obtain the covariance matrix for our Fisher analysis as a sum of eq. (5.3) and (5.4). In figure 4, we compare the derived statistical error (the square root of the diagonal part of the covariance matrix) and the estimated difference of the lensing power spectra between the mixed dark matter models considered here. Clearly, future wide field lensing surveys with 1500 square degrees can discriminate (or constrain) the light gravitino models. There are some certain degeneracies among the cosmological parameters, which we shall discuss in section 5.4.

We explore more realistic constraints by using priors expected from the cosmological parameter estimates from the Planck satellite mission. When we compute the Fisher matrix for the CMB, we use the Markov-Chain Monte-Carlo (MCMC) engine `COSMOMC` [60] for exploring cosmological parameter space. We consider the parameter constraints from the angular power spectra of temperature anisotropies, E-mode polarization, and their cross-correlation. For MCMC, in addition to $10^9 A_s, n_s, \Omega_c h^2$ and w_0, we adopt the baryon density

JHEP06(2014)162

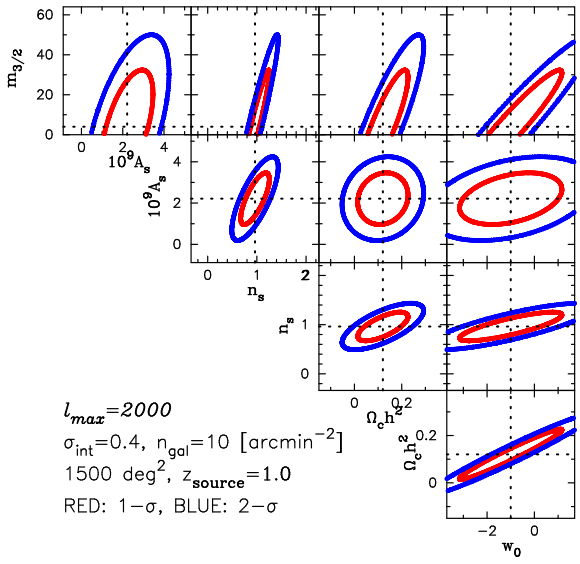

Figure 5. We show the cosmological constraints from lensing power spectrum alone. We consider the upcoming Subaru Hyper Suprime-Cam survey with an area of 1500 deg^2.

$\Omega_b h^2$, Hubble parameter h, and reionization optical depth τ as independent parameters. To examine the potential of lensing power spectrum to constrain $m_{3/2}$, we do not assume any prior on $m_{3/2}$ from the CMB. Assuming that the constraints from the CMB and the lensing power spectrum are independent of each other, we express the total Fisher matrix as

$$\boldsymbol{F} = \boldsymbol{F}_{\rm lensing} + \boldsymbol{F}_{\rm CMB}. \tag{5.6}$$

When we include the CMB priors in this way, we marginalize over the other cosmological parameters except $\boldsymbol{p} = (m_{3/2}, 10^9 A_s, n_s, \Omega_c h^2, w_0)$.

5.3 Forecast for future surveys

We provide the forecast for upcoming weak lensing surveys with an area coverage of more than a thousand square degrees. We use logarithmically spaced bins with $\Delta \log_{10} \ell = 0.1$ from $\ell = 100$ to 2000. We thus need a 14×14 covariance matrix of lensing power spectrum in the Fisher analysis. Our 1000 mock observations are sufficiently large to estimate the covariance matrix accurately.

Figure 5 shows the two-dimensional confidence contours for the Subaru Hyper Suprime-Cam (HSC) lensing survey.[2] We assume $n_{\rm gal} = 10$ arcmin^{-2}. The red circles show the constraints with 68 % confidence level (1σ) whereas the blue ones correspond to 95 % confidence level (2σ). The marginalized 1σ error for $m_{3/2}$ over other parameters is found to be ~ 18 eV.[3] Note that this is a constraint from the lensing survey alone. We also show

[2] http://www.naoj.org/Projects/HSC/j_index.html.

[3] One may think that figure 5 shows the marginalized 1σ error for $m_{3/2}$ should be ~ 30 eV. Here let us remind that the values of χ^2 corresponding to 68 % confidence level are different by a factor of ~ 2.3 between one and two degrees of freedom. Noting this point, we can obtain a marginalized 1σ error of $(32-4)/\sqrt{2.3} \sim 18$ eV.

JHEP06(2014)162

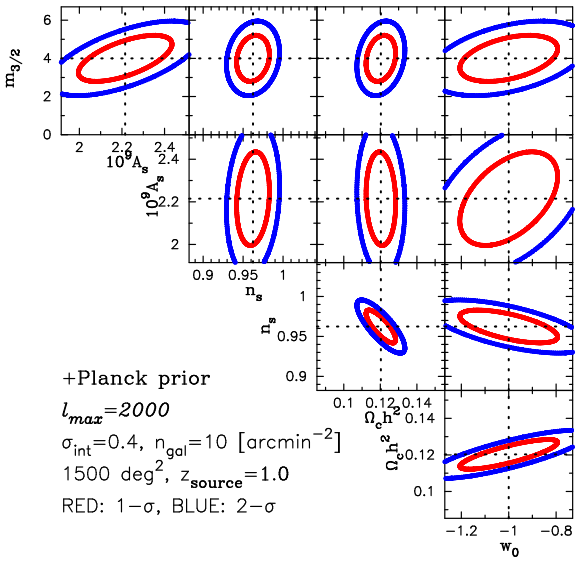

Figure 6. As for figure 5, but with the CMB priors described in section 5.2.

the forecast with the CMB priors in figure 6. The constraint on the gravitino mass is significantly improved in this case, because using the CMB data breaks some degeneracies among cosmological parameters, e.g. $10^9 A_s$ and $\Omega_c h^2$ [7]. It is impressive that we can derive constraint on the gravitino mass with a level of 1 eV by combining data from the HSC lensing survey and the Planck mission.

5.4 Degeneracy between light gravitino and massive neutrino

It is well known that massive neutrinos affect the lensing power spectrum in a similar way to the light gravitino; free-streaming of massive neutrinos suppress the growth of structure. At large length scales, the effect on $P_\delta(k)$ has been quantified by linear theory and extensions to first-order perturbation theory, e.g. [61, 62]. Probing the effect of massive neutrinos on $P_\delta(k)$ in the fully non-linear regime is still challenging, because it is difficult to include the relativistic species in N-body simulations [63–66]. In order to study the degeneracy between the light gravitino mass and the total mass of massive neutrinos in the cosmological parameter estimate, we utilize a fitting model of $P_\delta(k)$ that includes the effect of neutrinos [66].

Figure 7 shows the effect of massive neutrinos on the lensing power spectrum. There, we assume the mass of neutrino $m_{\nu,\mathrm{tot}} = 0.7\,\mathrm{eV}$, which is comparable to the current upper limits with 95% confidence [67–69]. We compare the lensing power spectrum with those of the light gravitino with $m_{3/2} = 4$ and 16 eV. As expected, massive neutrinos with $m_{\nu,\mathrm{tot}} = 0.7\,\mathrm{eV}$ cause a similar effect on the lensing power spectrum to that of the light gravitino. We see an appreciable difference in the range between the cut-off scales of the massive neutrino and the light gravitino (from $\ell = 10$ to $\ell = 1000$ in figure 7). On the other hand, the error in weak lensing survey is large at low multipole $\ell \lesssim 500$ (see figure 4). Apparently the weak lensing survey is not sensitive to the cut-off scale of the light gravitino. It would thus be difficult to break the degeneracy between the contribution of the light

JHEP06(2014)162

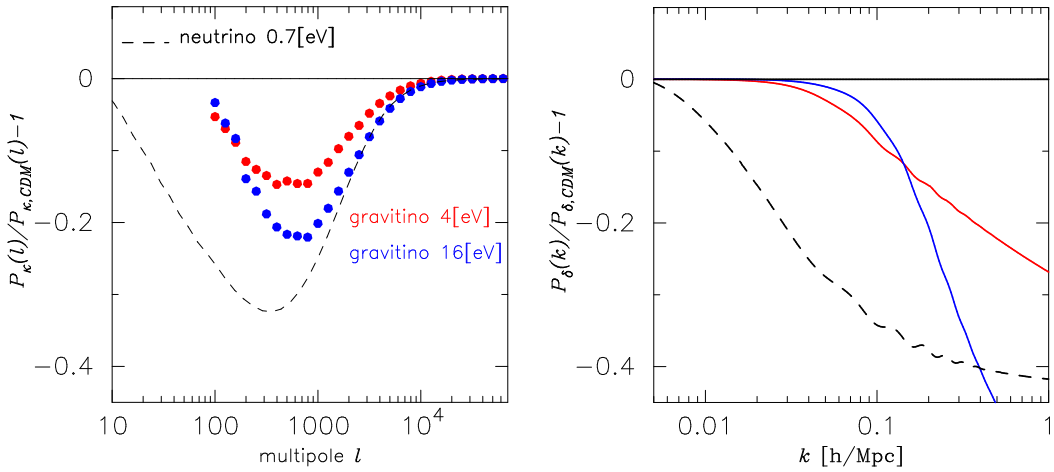

Figure 7. The effect of the light gravitino and massive neutrinos on the lensing power spectrum (left) and on the three dimensional linear matter power spectrum at $z = 0$ (right). In each panel, the dashed line shows the resulting lensing power spectrum calculated by the fitting model in [66] including the effect of massive neutrinos. We assume $m_{\nu,\mathrm{tot}} = 0.7\,\mathrm{eV}$. The points show the measured power spectra from our simulations in the case of $m_{3/2} = 4\,\mathrm{eV}$ (red) and $m_{3/2} = 16\,\mathrm{eV}$ (blue). We show these power spectra normalized by that for the pure CDM model.

gravitino and that of massive neutrinos by a weak lensing survey alone. We need other probes of the matter distribution at large length scales and at different epochs, such as galaxy clustering. For example, future galaxy redshift surveys are aimed at measuring the galaxy clustering at $k \sim 0.01 - 0.1\ h/\mathrm{Mpc}$. At the quasi-nonlinear length scales, the effect of massive neutrinos on $P_\delta(k)$ can be distinguishable from that of the light gravitino, as shown in the right panel of figure 7.

6 Summary and discussion

The gravitino mass is one of the fundamental parameters in SUSY theory that is directly related to the SUSY breaking energy scale. We focus on the gauge-mediated SUSY breaking model that generically predicts the existence of light gravitinos with $m_{3/2} \sim$eV-keV. Free-streaming of such light gravitino affects the matter distribution significantly, leaving characteristic suppression in the matter power spectrum at around $k \gtrsim 0.1\,\mathrm{h/Mpc}$. Such a nonlinear length scale is beyond the reach of the CMB anisotropy measurements. We show that observations of weak gravitational lensing can be used to probe the matter distribution at the relevant length scales and thus can be used to detect the imprints of the light gravitino.

We have explored cosmological constraints on the light gravitino mass from cosmic shear statistics. Our ray-tracing simulations have revealed that the conventional model for nonlinear correction to the matter power spectrum [49] does not work well for models with the light gravitino. The difference between the simulation results and the fitting formula is significant at $\ell \sim 1000$, where upcoming lensing surveys are aimed at measuring the power spectrum accurately. Using a large set of ray-tracing simulations, we have shown

JHEP06(2014)162

that the HSC like survey has a potential to determine the gravitino mass with an accuracy of $4 \pm 1\,\mathrm{eV}$ with the help of Planck CMB priors on the basic cosmological parameters.

Let us further discuss prospects for future lensing surveys. For the upcoming survey with 20000 deg^2 by the Large Synoptic Survey Telescope (LSST),[4] we will be able to use fainter galaxies for lensing analysis. Effectively the number of source galaxies will be larger. In this case, we can constrain on $m_{3/2}$ with a level of $4 \pm 0.6\,\mathrm{eV}$ assuming $n_{\mathrm{gal}} = 15$ arcmin^{-2}. Note that the constraint is tighter than the current one from the Lyman-α forest by a factor of ~ 10 [2], and also comparable to the forecast that utilizes CMB lensing [3]. We summarize the forecast of $m_{3/2}$ from upcoming weak lensing survey in figure 8. In the above discussion, we ignore the effects of massive neutrinos. The overall effect on the matter power spectrum can be similar to that of the light gravitino. We see an appreciable difference in the range between the cutoff-scales of massive neutrino and light gravitino. The weak lensing surveys alone are not able to distinguish the two effects. We expect that future galaxy redshift and/or CMB lensing surveys will help breaking the degeneracy by probing the matter power spectrum, and possibly its evolution, at (quasi-)nonlinear length scales.

Here, we take specific focus points in the minimal GMSB model to obtain the current and future LHC lower bound on the gravitino mass. As we mention in section 2, the LHC lower bound on the light gravitino mass is generically model-dependent. The ATLAS collaboration sets the lower bound on $\Lambda > 51\,\mathrm{TeV}$ with $M = 250\,\mathrm{TeV}$ and $N_5 = 3$ ($\mathbf{10} + \bar{\mathbf{10}}$ of SU(5)) fixed from the events with at least one tau lepton and no light lepton in 21 fb^{-1} of LHC 8 TeV run [23]. This can be interpreted as a lower bound on the gravitino mass $m_{3/2} > 3\,\mathrm{eV}$ through eq. (2.7), for the assumed perturbative coupling $|\lambda| < 1$. It is expected that the $\Lambda = 80\,\mathrm{TeV}$ is accessible even for $N_5 = 5$ with the use of the multi-lepton modes in about 15 fb^{-1} of LHC 14 TeV run [19]. We would like to emphasize that the latter constraint is the minimum of the LHC lower bound from the theoretical (model-building) point of view. In order to derive conservative and model-independent constraints on the gravitino mass from the collider experiments, we should take maximum value of N_5 and $|\lambda| x$ (see eqs. (2.2), (2.5) and (2.7)). For the successful grand unification of the gauge couplings, the number of messenger N_5 needs to be at most five, $N_5 \leq 5$. Furthermore, the stability of the SUSY breaking vacuum requires $|\lambda| x > 1.4$ [24].[5] Therefore, by setting $N_5 = 5$ and $|\lambda| x = 1.4$, we obtain the conservative and rather model-independent lower bound on the light gravitino mass. An exciting implication of this is that virtually all of the GMSB models with $m_{3/2} < 5\,\mathrm{eV}$ can be probed in 15 fb^{-1} of LHC 14 TeV run. We summarize the used values of parameters in table 3.

Ultimately, the International Linear Collider (ILC) experiment has a potential to determine the gravitino mass. When the next lightest supersymmetric particle is stau, its lifetime is proportional to the gravitino mass squared. By measuring the distribution of the impact parameter, one can evaluate the stau lifetime and hence the gravitino mass [70].[6]

[4] http://www.lsst.org/lsst/.

[5] Considering the thermal transition of the SUSY breaking vacuum leads to more stringent constraint on $|\lambda| x$ [25]. Here, we consider only quantum (zero-temperature) transition to be conservative.

[6] To this end, the center of mass energy should exceed two time the stau mass and the background events should be effectively eliminated. However, this may be challenging for the present design of the ILC in the case of the heavy stau for a given gravitino mass, i.e. large N_5 and λx.

JHEP06(2014)162

focus point	fixed GMSB parameters	LHC	Λ	$m_{3/2}$
current	$M = 250\,\text{TeV}, N_5 = 3, \lvert\lambda\rvert = 1$	$21\,\text{fb}^{-1}$ at $\sqrt{s} = 8\,\text{TeV}$	$\Lambda = 51\,\text{TeV}$	$m_{3/2} = 3\,\text{eV}$
future	$\lvert\lambda\rvert x = 1.4, N_5 = 5$	$15\,\text{fb}^{-1}$ at $\sqrt{s} = 14\,\text{TeV}$	$\Lambda = 80\,\text{TeV}$	$m_{3/2} = 5\,\text{eV}$

Table 3. Summary of the focus points for the GMSB model described in the text. The current focus point corresponds to the current lower bound on Λ reported in [23]. In the future focus point, the GMSB parameters are set such that they minimize the gravitino mass for fixed Λ while stabilizing the SUSY breaking vacuum. The future LHC reach is taken from [19].

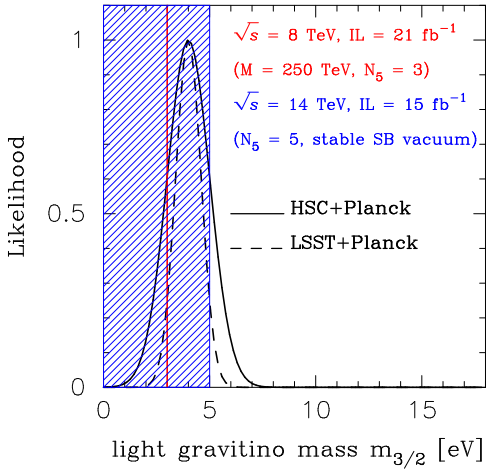

Figure 8. The likelihood distribution of $m_{3/2}$ expected by future weak lensing surveys. We have used the binned lensing power spectrum with the CMB prior for this figure. The solid line corresponds to the Hyper Suprime-Cam survey and the dashed one is for Large Synoptic Survey Telescope. The vertical lines show the current/future focus points of the GMSB model at the LHC (table 3). In the near-future LHC, all GMSB models with $m_{3/2} < 5\,\text{eV}$ (shaded region) can be probed if they involve the stable SUSY breaking (SB) vacuum and the successful grand unification.

Combining cosmological and collider searches together, we will reach the conclusion about the GMSB model.

Acknowledgments

A.K. would like to thank M. Ibe, S. Matsumoto, and T.T. Yanagida for useful discussions. M.S. appreciates M. Sato for kindly providing us the set of simulations. Numerical computations for the present work have been carried out on Cray XC30 at Center for Computational Astrophysics, CfCA, of National Astronomical Observatory of Japan, and in part under the Interdisciplinary Computational Science Program in Center for Computational Sciences, University of Tsukuba. This work is supported in part by JSPS Research Fellowship for Young Scientists (A.K. and M.S.) and by World Premier International Research Center Initiative, MEXT, Japan.

JHEP06(2014)162

References

[1] S.P. Martin, *A supersymmetry primer*, hep-ph/9709356 [INSPIRE].

[2] M. Viel, J. Lesgourgues, M.G. Haehnelt, S. Matarrese and A. Riotto, *Constraining warm dark matter candidates including sterile neutrinos and light gravitinos with WMAP and the Lyman-α forest*, *Phys. Rev.* **D 71** (2005) 063534 [astro-ph/0501562] [INSPIRE].

[3] K. Ichikawa, M. Kawasaki, K. Nakayama, T. Sekiguchi and T. Takahashi, *Constraining light gravitino mass from cosmic microwave background*, *JCAP* **08** (2009) 013 [arXiv:0905.2237] [INSPIRE].

[4] D.J. Bacon, R.J. Massey, A.R. Refregier and R.S. Ellis, *Joint cosmic shear measurements with the Keck and William Herschel Telescopes*, *Mon. Not. Roy. Astron. Soc.* **344** (2003) 673 [astro-ph/0203134] [INSPIRE].

[5] T. Hamana et al., *Cosmic shear statistics in the Suprime-Cam 2.1 Square Degree Field: Constraints on Ω_m and σ_8*, *Astrophys. J.* **597** (2003) 98 [astro-ph/0210450] [INSPIRE].

[6] J. Benjamin et al., *Cosmological Constraints From the 100-deg^2 Weak-Lenging Survey*, *Mon. Not. Roy. Astron. Soc.* **381** (2007) 702 [astro-ph/0703570] [INSPIRE].

[7] M. Kilbinger et al., *CFHTLenS: Combined probe cosmological model comparison using 2D weak gravitational lensing*, *Mon. Not. Roy. Astron. Soc.* **430** (2013) 2200 [arXiv:1212.3338] [INSPIRE].

[8] M. Dine and W. Fischler, *A Phenomenological Model of Particle Physics Based on Supersymmetry*, *Phys. Lett.* **B 110** (1982) 227 [INSPIRE].

[9] C.R. Nappi and B.A. Ovrut, *Supersymmetric Extension of the* SU(3) × SU(2) × U(1) *Model*, *Phys. Lett.* **B 113** (1982) 175 [INSPIRE].

[10] L. Álvarez-Gaumé, M. Claudson and M.B. Wise, *Low-Energy Supersymmetry*, *Nucl. Phys.* **B 207** (1982) 96 [INSPIRE].

[11] M. Dine and A.E. Nelson, *Dynamical supersymmetry breaking at low energies*, *Phys. Rev.* **D 48** (1993) 1277 [hep-ph/9303230] [INSPIRE].

[12] M. Dine, A.E. Nelson and Y. Shirman, *Low energy dynamical supersymmetry breaking simplified*, *Phys. Rev.* **D 51** (1995) 1362 [hep-ph/9408384] [INSPIRE].

[13] M. Dine, A.E. Nelson, Y. Nir and Y. Shirman, *New tools for low energy dynamical supersymmetry breaking*, *Phys. Rev.* **D 53** (1996) 2658 [hep-ph/9507378] [INSPIRE].

[14] B.C. Allanach, *SOFTSUSY: a program for calculating supersymmetric spectra*, *Comput. Phys. Commun.* **143** (2002) 305 [hep-ph/0104145] [INSPIRE].

[15] H. Baer, P.G. Mercadante, F. Paige, X. Tata and Y. Wang, *LHC reach for gauge mediated supersymmetry breaking models via prompt photon channels*, *Phys. Lett.* **B 435** (1998) 109 [hep-ph/9806290] [INSPIRE].

[16] H. Baer, P.G. Mercadante, X. Tata and Y.-l. Wang, *Reach of the CERN large hadron collider for gauge-mediated supersymmetry breaking models*, *Phys. Rev.* **D 62** (2000) 095007 [hep-ph/0004001] [INSPIRE].

[17] ATLAS collaboration, *Expected Performance of the ATLAS Experiment — Detector, Trigger and Physics*, arXiv:0901.0512 [INSPIRE].

[18] ATLAS collaboration, *Expected Performance of the ATLAS Detector in GMSB Models with Tau Final States*, PoS(HCP2009)073 [arXiv:1002.0944] [INSPIRE].

JHEP06(2014)162

[19] E. Nakamura and S. Shirai, *Discovery Potential for Low-Scale Gauge Mediation at Early LHC*, *JHEP* **03** (2011) 115 [arXiv:1010.5995] [INSPIRE].

[20] ATLAS collaboration, *Search for events with large missing transverse momentum, jets and at least two tau leptons in 7 TeV proton-proton collision data with the ATLAS detector*, *Phys. Lett.* **B 714** (2012) 180 [arXiv:1203.6580] [INSPIRE].

[21] ATLAS collaboration, *Search for supersymmetry with jets, missing transverse momentum and at least one hadronically decaying τ lepton in proton-proton collisions at $\sqrt{s} = 7$ TeV with the ATLAS detector*, *Phys. Lett.* **B 714** (2012) 197 [arXiv:1204.3852] [INSPIRE].

[22] ATLAS collaboration, *Search for Supersymmetry in Events with Large Missing Transverse Momentum, Jets and at Least One Tau Lepton in 7 TeV Proton-Proton Collision Data with the ATLAS Detector*, *Eur. Phys. J.* **C 72** (2012) 2215 [arXiv:1210.1314] [INSPIRE].

[23] ATLAS collaboration, *Search for Supersymmetry in Events with Large Missing Transverse Momentum, Jets, and at Least One Tau Lepton in 21 fb^{-1} of $\sqrt{s} = 8$ TeV Proton-Proton Collision Data with the ATLAS Detector* ATLAS-CONF-2013-026 (2013).

[24] J. Hisano, M. Nagai, M. Senami and S. Sugiyama, *Stability of Metastable Vacua in Gauge Mediated SUSY Breaking Models with Ultra Light Gravitino*, *Phys. Lett.* **B 659** (2008) 361 [arXiv:0708.3340] [INSPIRE].

[25] J. Hisano, M. Nagai, S. Sugiyama and T.T. Yanagida, *Upperbound on Squark Masses in Gauge-Mediation Model with Light Gravitino*, *Phys. Lett.* **B 665** (2008) 237 [arXiv:0804.2957] [INSPIRE].

[26] T. Moroi, H. Murayama and M. Yamaguchi, *Cosmological constraints on the light stable gravitino*, *Phys. Lett.* **B 303** (1993) 289 [INSPIRE].

[27] E. Pierpaoli, S. Borgani, A. Masiero and M. Yamaguchi, *Formation of cosmic structures in a light gravitino dominated universe*, *Phys. Rev.* **D 57** (1998) 2089 [astro-ph/9709047] [INSPIRE].

[28] J. Preskill, M.B. Wise and F. Wilczek, *Cosmology of the Invisible Axion*, *Phys. Lett.* **B 120** (1983) 127 [INSPIRE].

[29] L.F. Abbott and P. Sikivie, *A Cosmological Bound on the Invisible Axion*, *Phys. Lett.* **B 120** (1983) 133 [INSPIRE].

[30] M. Dine and W. Fischler, *The Not-So-Harmless Axion*, *Phys. Lett.* **B 120** (1983) 137 [INSPIRE].

[31] S. Dimopoulos, G.F. Giudice and A. Pomarol, *Dark matter in theories of gauge-mediated supersymmetry breaking*, *Phys. Lett.* **B 389** (1996) 37 [hep-ph/9607225] [INSPIRE].

[32] J. Fan, J. Thaler and L.-T. Wang, *Dark matter from dynamical SUSY breaking*, *JHEP* **06** (2010) 045 [arXiv:1004.0008] [INSPIRE].

[33] T.T. Yanagida and K. Yonekura, *A Conformal Gauge Mediation and Dark Matter with Only One Mass Parameter*, *Phys. Lett.* **B 693** (2010) 281 [arXiv:1006.2271] [INSPIRE].

[34] T.T. Yanagida, N. Yokozaki and K. Yonekura, *Higgs Boson Mass in Low Scale Gauge Mediation Models*, *JHEP* **10** (2012) 017 [arXiv:1206.6589] [INSPIRE].

[35] A. Kamada, N. Yoshida, K. Kohri and T. Takahashi, *Structure of Dark Matter Halos in Warm Dark Matter models and in models with Long-Lived Charged Massive Particles*, *JCAP* **03** (2013) 008 [arXiv:1301.2744] [INSPIRE].

JHEP06(2014)162

[36] M. Ibe, R. Sato, T.T. Yanagida and K. Yonekura, *Gravitino Dark Matter and Light Gluino in an R-invariant Low Scale Gauge Mediation*, *JHEP* **04** (2011) 077 [arXiv:1012.5466] [INSPIRE].

[37] A. Lewis, A. Challinor and A. Lasenby, *Efficient computation of Cosmic Microwave Background anisotropies in closed Friedmann-Robertson-Walker models*, *Astrophys. J.* **538** (2000) 473 [astro-ph/9911177] [INSPIRE].

[38] PLANCK collaboration, P.A.R. Ade et al., *Planck 2013 results. XVI. Cosmological parameters*, arXiv:1303.5076 [INSPIRE].

[39] M. Bartelmann and P. Schneider, *Weak gravitational lensing*, *Phys. Rept.* **340** (2001) 291 [astro-ph/9912508] [INSPIRE].

[40] D. Munshi, P. Valageas, L. Van Waerbeke and A. Heavens, *Cosmology with Weak Lensing Surveys*, *Phys. Rept.* **462** (2008) 67 [astro-ph/0612667] [INSPIRE].

[41] D.N. Limber, *The Analysis of Counts of the Extragalactic Nebulae in Terms of a Fluctuating Density Field. II*, *Astrophys. J.* **119** (1954) 655 [INSPIRE].

[42] N. Kaiser, *Weak gravitational lensing of distant galaxies*, *Astrophys. J.* **388** (1992) 272 [INSPIRE].

[43] B. Jain, U. Seljak and S.D.M. White, *Ray-tracing simulations of weak lensing by large scale structure*, *Astrophys. J.* **530** (2000) 547 [astro-ph/9901191] [INSPIRE].

[44] S. Hilbert, J. Hartlap, S.D.M. White and P. Schneider, *Ray-tracing through the Millennium Simulation: Born corrections and lens-lens coupling in cosmic shear and galaxy-galaxy lensing*, *Astron. Astrophys.* **499** (2009) 31 [arXiv:0809.5035] [INSPIRE].

[45] M. Sato et al., *Simulations of Wide-Field Weak Lensing Surveys I: Basic Statistics and Non-Gaussian Effects*, *Astrophys. J.* **701** (2009) 945 [arXiv:0906.2237] [INSPIRE].

[46] J.A. Peacock and S.J. Dodds, *Non-linear evolution of cosmological power spectra*, *Mon. Not. Roy. Astron. Soc.* **280** (1996) L19 [astro-ph/9603031] [INSPIRE].

[47] VIRGO CONSORTIUM collaboration, R.E. Smith et al., *Stable clustering, the halo model and nonlinear cosmological power spectra*, *Mon. Not. Roy. Astron. Soc.* **341** (2003) 1311 [astro-ph/0207664] [INSPIRE].

[48] K. Heitmann, M. White, C. Wagner, S. Habib and D. Higdon, *The Coyote Universe I: Precision Determination of the Nonlinear Matter Power Spectrum*, *Astrophys. J.* **715** (2010) 104 [arXiv:0812.1052] [INSPIRE].

[49] R. Takahashi, M. Sato, T. Nishimichi, A. Taruya and M. Oguri, *Revising the Halofit Model for the Nonlinear Matter Power Spectrum*, *Astrophys. J.* **761** (2012) 152 [arXiv:1208.2701] [INSPIRE].

[50] V. Springel, *The Cosmological simulation code GADGET-2*, *Mon. Not. Roy. Astron. Soc.* **364** (2005) 1105 [astro-ph/0505010] [INSPIRE].

[51] M.J. White and W. Hu, *A New algorithm for computing statistics of weak lensing by large scale structure*, *Astrophys. J.* **537** (2000) 1 [astro-ph/9909165] [INSPIRE].

[52] T. Hamana and Y. Mellier, *Numerical study of statistical properties of the lensing excursion angles*, *Mon. Not. Roy. Astron. Soc.* **327** (2001) 169 [astro-ph/0101333] [INSPIRE].

[53] V. Avila-Reese, P. Colin, O. Valenzuela, E. D'Onghia and C. Firmani, *Formation and structure of halos in a warm dark matter cosmology*, *Astrophys. J.* **559** (2001) 516 [astro-ph/0010525] [INSPIRE].

JHEP06(2014)162

[54] T. Eifler, P. Schneider and J. Hartlap, *Dependence of cosmic shear covariances on cosmology — Impact on parameter estimation*, *Astron. Astrophys.* **502** (2009) 721 [arXiv:0810.4254] [INSPIRE].

[55] A. Cooray and W. Hu, *Power spectrum covariance of weak gravitational lensing*, *Astrophys. J.* **554** (2001) 56 [astro-ph/0012087] [INSPIRE].

[56] M. Sato and T. Nishimichi, *Impact of the non-Gaussian covariance of the weak lensing power spectrum and bispectrum on cosmological parameter estimation*, *Phys. Rev.* **D 87** (2013) 123538 [arXiv:1301.3588] [INSPIRE].

[57] M. Takada and M.J. White, *Tomography of lensing cross-power spectra*, *Astrophys. J.* **601** (2004) L1 [astro-ph/0311104] [INSPIRE].

[58] S. Miyazaki et al., *Searching for dark matter halos in the Suprime-CAM 2 Square Degree Field*, *Astrophys. J.* **580** (2002) L97 [astro-ph/0210441] [INSPIRE].

[59] R. Mandelbaum, U. Seljak, G. Kauffmann, C.M. Hirata and J. Brinkmann, *Galaxy halo masses and satellite fractions from galaxy-galaxy lensing in the Sloan Digital Sky Survey: stellar mass, luminosity, morphology and environment dependencies*, *Mon. Not. Roy. Astron. Soc.* **368** (2006) 715 [astro-ph/0511164] [INSPIRE].

[60] A. Lewis and S. Bridle, *Cosmological parameters from CMB and other data: A Monte Carlo approach*, *Phys. Rev.* **D 66** (2002) 103511 [astro-ph/0205436] [INSPIRE].

[61] J.R. Bond, G. Efstathiou and J. Silk, *Massive Neutrinos and the Large Scale Structure of the Universe*, *Phys. Rev. Lett.* **45** (1980) 1980 [INSPIRE].

[62] S. Saito, M. Takada and A. Taruya, *Impact of massive neutrinos on nonlinear matter power spectrum*, *Phys. Rev. Lett.* **100** (2008) 191301 [arXiv:0801.0607] [INSPIRE].

[63] J. Brandbyge and S. Hannestad, *Grid Based Linear Neutrino Perturbations in Cosmological N-body Simulations*, *JCAP* **05** (2009) 002 [arXiv:0812.3149] [INSPIRE].

[64] J. Brandbyge, S. Hannestad, T. Haugbolle and B. Thomsen, *The Effect of Thermal Neutrino Motion on the Non-linear Cosmological Matter Power Spectrum*, *JCAP* **08** (2008) 020 [arXiv:0802.3700] [INSPIRE].

[65] M. Viel, M.G. Haehnelt and V. Springel, *The effect of neutrinos on the matter distribution as probed by the Intergalactic Medium*, *JCAP* **06** (2010) 015 [arXiv:1003.2422] [INSPIRE].

[66] S. Bird, M. Viel and M.G. Haehnelt, *Massive Neutrinos and the Non-linear Matter Power Spectrum*, *Mon. Not. Roy. Astron. Soc.* **420** (2012) 2551 [arXiv:1109.4416] [INSPIRE].

[67] B.A. Reid et al., *Cosmological Constraints from the Clustering of the Sloan Digital Sky Survey DR7 Luminous Red Galaxies*, *Mon. Not. Roy. Astron. Soc.* **404** (2010) 60 [arXiv:0907.1659] [INSPIRE].

[68] S. Saito, M. Takada and A. Taruya, *Neutrino mass constraint from the Sloan Digital Sky Survey power spectrum of luminous red galaxies and perturbation theory*, *Phys. Rev.* **D 83** (2011) 043529 [arXiv:1006.4845] [INSPIRE].

[69] G.-B. Zhao et al., *The clustering of galaxies in the SDSS-III Baryon Oscillation Spectroscopic Survey: weighing the neutrino mass using the galaxy power spectrum of the CMASS sample*, *Mon. Not. Roy. Astron. Soc.* **436** (2013) 2038 [arXiv:1211.3741] [INSPIRE].

[70] S. Matsumoto and T. Moroi, *Studying Very Light Gravitino at the ILC*, *Phys. Lett.* **B 701** (2011) 422 [arXiv:1104.3624] [INSPIRE].

JHEP06(2014)162